Indian Journal of Pure & Applied Physics
Vol. 61, January 2023, pp. 67-74
DOI: 10.56042/ijpap.v61i1.65453

Core Loss Study of Different Structures of Terfenol-D Rods

Qiang Liu & Xiping He*

School of Physics and Information Technology, Shaanxi Normal University, No. 620 West Chang'an Street, Chang'an District, Xi'an, Shaanxi Province, 710 119, China

Received 11 August 2022; accepted 21 December 2022

To efficiently use Terfenol-D rods, six of its structures were studied. Finite element analysis was used to estimate and compare the hysteresis, eddy current, and coil resistance losses of the six Terfenol-D rods. The loss factors of the rods were calculated and analyzed. Furthermore, three structures of Terfenol-D rods were manufactured, and the loss factors of the rods were measured. The results showed that an untreated rod had the largest hysteresis and eddy current losses on the outer diameter surface, and the overall hysteresis loss of the rod was the smallest. Compared with the untreated rod, the eddy current and hysteresis losses on the outer diameter surface of sliced and slit rods reduced, the overall hysteresis loss of sliced and slit rods increased, and the overall eddy current loss of sliced rods reduced; the hysteresis and eddy current losses on the surface of the sliced rods were less than that of the slit rods, and the overall eddy current loss of the sliced rods was less than that of the slit rods; moreover, the eddy current loss of each rod was larger than its hysteresis loss. The numerical calculation values of the coil resistance loss basically agreed with the theoretical calculation values. The finite element simulation calculation values of the loss factors of the Terfenol-D rods agreed with the experimental test values.

Keywords: Terfenol-D rod; Hysteresis loss; Eddy current loss; Coil resistance loss; Finite element calculation

1 Introduction

Ultrasonic waves are widely used in the fields of industry, agriculture, medicine, and environmental protection. A transducer converts electrical signals to the required ultrasonic waves, so it is a critical component to determine the performance of an ultrasonic vibration system. Currently, the most commonly used transducers in the industry are piezoelectric transducer and the magnetostrictive transducers[1]. Compared with piezoelectric ceramic materials, giant magnetostrictive materials (GMM) have high thermal conductivity, large magnetostrictive coefficient, high-power density, lower sound velocity; no overheating failure problems, fast response speed, and strong load capacity; thus, GMM is an excellent functional material for developing high-power, large amplitude, and wideband ultrasonic processing systems. The superior dynamic features of GMM make them suitable for many applications, such as transducers, sensors, actuators, vibration energy harvesting[2-5].

A transducer converts electromagnetic energy to mechanical energy. Be sides, thermal power losses are generated when driven by a high-frequency alternating magnetic field. The presence of thermal power loss can alter the magnetostrictive coefficientof the Terfenol-D, thereby reducing the driving efficiency of the transducer. Kwak *et al.*[6] studied the influence of temperature on the displacement characteristics of giant magnetostrictive actuators. The heat generated by an excitation coil will cause a thermal strain of Terfenol-D and make it difficult to control the precise position of the actuator. Zeng *et al.*[7] proposed a hysteresis loss calculation method based on the Jiles–Atherton hysteresis model and electromagnetic field finite element analysis, which coupled the hysteresis loss to the thermal analysis of a giant magnetostrictive transducer. Takahashi *et al.*[8] calculated the total loss by measuring the temperature of a giant magnetostrictive actuator and fitted the total loss of the actuator at different frequencies to obtain the coil resistance and Terfenol-D rods' losses. Engdahl *et al.*[9] simulated and analyzed losses of a giant magnetostrictive actuator and obtained the resistance loss of the coil and eddy current and hysteresis losses of the Terfenol-D rod. The core loss of the Terfenol-D rod is the primary energy loss of a giant magnetostrictive transducer.

Xu *et al.*[10] established a dynamic eddy current loss model of the Terfenol-D. The model was shown to predict the dynamic magnetostrictive effect of Terfenol-D under alternating magnetic field and

*Corresponding author: (E-mail: hexiping@snnu.edu.cn)

prestress. It was found that the eddy current loss gradually dominated the energy loss as the excitation frequency increased, whereas anomalous loss is not obvious. Talebian *et al*.[11] studied the classic and excess eddy current losses of Terfenol-D and determined the influence of the magnetic field frequency, peak magnetic flux density, and Terfenol-D rod diameter on the eddy current loss. Yamamoto *et al.*[12] investigated the hysteresis loss of Terfenol-D rod under compressive stress, the hysteresis loss increased monotonically with the increasing applied pressure. Meng *et al*.[13] investigated the magnetic energy loss and frequency dependence of TbDyFe/epoxy composites. The main losses were hysteresis loss of composites and eddy current loss of the monolithic TbDyFe alloy. Stillesjo *et al*.[14] analyzed different power losses of a giant magnetostrictive transducer with a 10-A driving current and 21-kHz frequency based on a dynamic model. The main heating was hysteresis loss. Huang *et al*.[15] sliced Terfenol-D rod along different directions into several square annular samples, analyzed the influence of material magnetization direction on loss, and measured magnetic energy loss under different frequencies and magnetic flux density. At present, the Terfenol-D rod is mainly sliced or slit to reduce eddy current loss.

He *et al*.[16] proposed a simple geometric method to calculate the number of slits for radial uniform slit processing. Tang *et al*.[17] proposed an analytical approach to estimate the cross sectional magnetic field distribution of Terfenol-D rods. Numerical evaluation and experiments showed that eddy current should be considered when either the nonuniformity error or the effective magnetic field strength error exceeded 5%. The Terfenol-D rod should be sliced. Teng *et al*.[18] proposed a digital slot on a Terfenol-D rod to reduce eddy current loss. The eddy current loss of the digital slot Terfenol-D rod was 78.5% lower than that of an untreated rod. Tao *et al*.[19] compared and analyzed the influence of the eddy current loss of Terfenol-D rod with monolithic and laminated structures on material impedance and vibration output characteristics. The results showed that the Terfenol-D rod with a laminated structure had higher eddy current cutoff frequency and minor eddy current loss. Gandomzadeh *et al*.[20] investigated the influence of nickel core geometry on the behavioral performance of ultrasonic transducer by using the finite element software. The structure size, working frequency, and magnetic flux density of Terfenol-D affect its core loss[21].

In this study, six structures of Terfenol-D rods were investigated. The hysteresis, eddy current, and coil resistance losses of several Terfenol-D rods were simulated and analyzed using the complex permeability of Terfenol-D in COMSOL Multiphysics 5.4, and the loss factors of the corresponding structural rods were calculated. Three types of Terfenol-D rods were manufactured, and their loss factors were tested.

2 Terfenol-D Rods with Several Structures

Because of the relatively small resistivity of Terfenol-D, severe eddy currents were generated when driven by a high-frequency alternating magnetic field. The presence of eddy currents increased the energy loss and reduced the driving efficiency of a transducer. A Terfenol-D rod was cut and bonded to improve the working frequency value, and a laminate thickness was close to or less than the "penetration depth" for normal operation. The limit working frequency of Terfenol-D rod can be calculated as follows:

$$f_{\max} = \frac{\rho_g}{\pi \delta_s^2 \mu_0 \mu_r} \quad ...(1)$$

Where ρ_g, δ_s, u_0, and u_r are the resistivity, skin depth, vacuum permeability, and relative permeability, respectively.

The dimensions of all Terfenol-D rods were the same; the outer diameter D = 18 mm, inner diameter d = 6 mm, and length l_g = 21.5 mm. The working frequency was 20 kHz. According to Eq. (1), the skin depth of the Terfenol-D rod was 1.2 mm, which was much smaller than the diameter of the Terfenol-D rod. Therefore, the Terfenol-D rod was cut into sheets with a 1.2 mm laminate thickness. The number of the radial slits of the Terfeol-D rod was calculated at the working frequency [16]. The epoxy resin thickness in the slits of the Terfenol-D rod was 0.4 mm, the Terfenol-D rods were bonded to the epoxy resin after being sliced or slit. Several Terfenol-D rods were previously designed[22], and the improved Terfenol-D rods with six structures are shown in Fig. 1. The untreated one is without cutting treatment (Fig. 1(a)); radial slit—first calculate the number of slits, then cut the slit along the outer diameter (the slit is 2 mm away from the inner diameter of the rod), and fill the slit with epoxy resin (Fig. 1(b)) radial cut and bonded (Fig.1(c)) according to the calculated number of slits, the Terfenol-D rod is cut along the outer

diameter to the inner diameter, and then bonded with epoxy resin; sliced and grooved (Fig. 1(d)) slice the Terfenol-D rod along the *X* direction (the thickness of the laminate and distance between the slit and the inner edge of the Terfenol-D rod are both 1.2 mm) and machine a groove in the middle of the rod along the *Y*-direction and then bond them together with insulating adhesive; sliced treatment (Fig. 1(e)) cut the Terfenol-D rod into sheets, with a laminate thickness of 1.2 mm, which are then bonded using epoxy resin; slicing at both ends (Fig. 1(f)) slice in the *Z*-direction from the upper end to 6 mm from the lower end, and then the lower end of Terfenol-D rods are sliced 4 mm upward, followed by cutting the lower end of the rod in the *Z*-direction to a distance of 6 mm from the upper end, then slicing the upper end of the Terfenol-D rod down 4 mm. The connecting parts between the slices were staggered in turn, and liquid epoxy resin was allowed to fill the slits from the other end under pressure and cure. It is an effective method to control the eddy currents and ensure the rod's integrity. The sliced rods include sliced and grooved (Fig. 1(d)), sliced (Fig. 1(e)), and sliced at both ends (Fig. 1(f)), slit rods include radial slit (Fig. 1(b)), and radial cut and bonded (Fig. 1(c)).

3 Simulation Calculation of Terfenol-D Rod

A giant magnetostrictive transducer generates ultrasonic vibration under the action of a high-frequency alternating magnetic field. In the magnetization process under an external magnetic field, the transducer will generatethe core loss of the Terfenol-D rod as well as the resistance loss of the coil. The core loss mainly includes the hysteresis and eddy current losses, which will be converted into heat

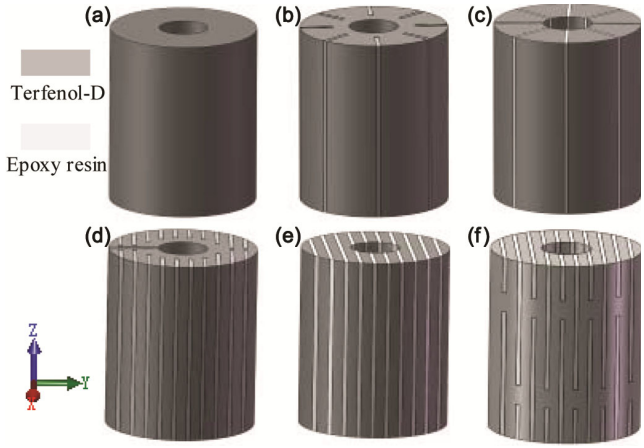

Fig. 1 — Structural diagram of different Terfenol-D rods. (a) Untreated; (b) Radial slit; (c) Radial cut and bonded; (d) Sliced and grooved; (e) Sliced; (f) Sliced at both ends.

to increase the temperature of the giant magnetostrictive transducer. The core loss of the Terfenol-D rod is the main energy loss of the giant magnetostrictive transducer.

The magnetic induction intensity *B* lags behind the magnetic field intensity *H*, there is a phase difference α, which is called the loss angle. In the alternating magnetic field, the complex permeability of the Terfenol-D rod is expressed as follows:

$$\mu = \frac{1}{\mu_0}\frac{B}{H} = \frac{B_m}{\mu_0 H_m} e^{-j\alpha} = \mu_r - i\mu_i \quad ...(2)$$

Where B_m is the peak magnetic induction intensity, H_m is the peak magnetic field intensity, μ_r and μ_i are the real and imaginary parts of the complex magnetic permeability, respectively; μ_r describes the stored capacity of magnetic energy during dynamic magnetization; μ_i represents the magnetic energy losses due to the magnetic dipole moment of the material under the action of the magnetic field.

In COMSOL Multiphysics 5.4, there are two methods to simulate and calculate hysteresis[23]. One is calculated by using the relative permeability of the complex value in frequency domain; the other is calculated by using the Jiles-Atherton vector hysteresis model in time domain, which needs to know five physical parameters. Comparatively speaking, the latter is cumbersome, and the amount of calculation is large. The J-A model is rarely used in practical engineering. Therefore, in this study, based on the complex permeability of Terfenol-D measured in the literature[24], the hysteresis loss of the rods was directly simulated and calculated with the first method.

Several models of Terfenol-D rods were built in Solid Works and imported into COMSOL Multiphysics 5.4. The transducer comprises a coil, a Terfenol-D rod, and an air domain outside the coil, the air domain is not shown in the figure. A schematic of the transducer is shown in Fig. 2.

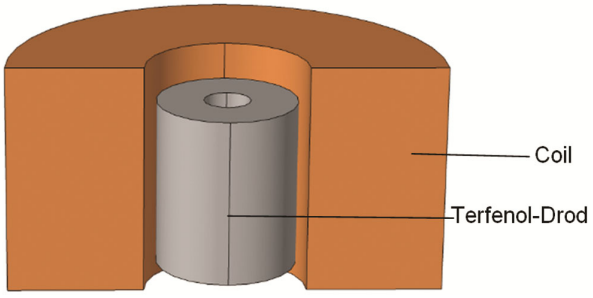

Fig. 2 — Schematic of a giant magnetostrictive transducer.

The material parameters of Terfenol-D as follows: electrical conductivity σ_g = 1.894×10^6 S/m, dielectric constant ε_r = 1, complex permeability μ = 21.9 + 18.21i; the default conductivity of air is 0 S/m, the conductivity is changed to 1 S/m to improve the stability of the solution, the conductivity of Terfenol-D is much larger than that of air. The error caused by this small conductivity can be ignored.

The coil settings are as follows: the conductor model was set as homogenized multiple-turns, the coil type was set as numeric, coil excitation was set as current, coil current was 1 A, and the number of coil turns was 350, frequency of the excitation coil was 20 kHz. In this study, some parameters, including the wire type, cross sectional wire area, wire length, number of turns, air gap between the coil and Terfenol-D rod, frequency, and current were assumed to be constant.

Taking Terfenol-D rod with the largest number of grid units as an example, Fig. 3 shows the grid diagram of sliced rods at both ends. The computation time for symmetrical model is much less compared to the full model because the total number of mesh decreases drastically. The amount of the nodes and volume grid elements are 11671, 58049, respectively, and the air field outside the rod and coil is not displayed. Then, frequency domain analysis was carried out in COMSOL Multiphysics 5.4.

The hysteresis and eddy current losses distributions of Terfenol-D rods with different structures were obtained in the 3D plot group of the results. Fig. 4 shows the hysteresis loss distribution of the Terfenol-D rods with different structures. Based on the analysis results, the untreated Terfenol-D rod (Fig. 4(a)) had the largest hysteresis loss on the outer diameter surface; the hysteresis loss on the outer diameter

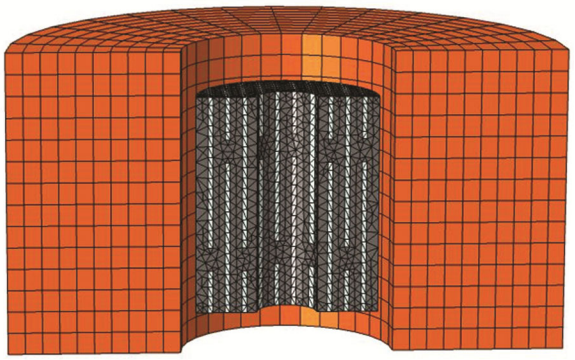

Fig. 3 — Grid diagram of sliced at both ends Terfenol-D rod.

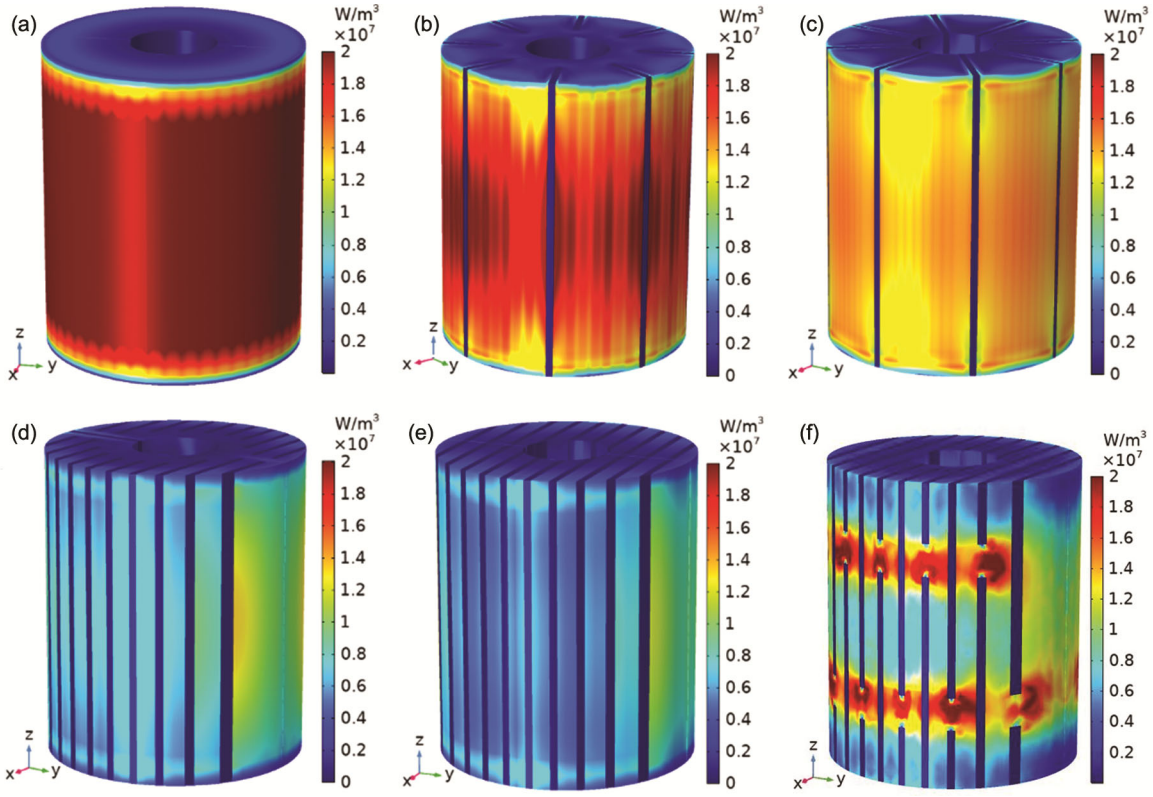

Fig. 4 — Hysteresis loss distribution diagram of Terfenol-D rods. (a) Untreated; (b) Radial slit; (c) Radial cut and bonded; (d) Sliced and grooved; (e) Sliced; (f) Sliced at both ends.

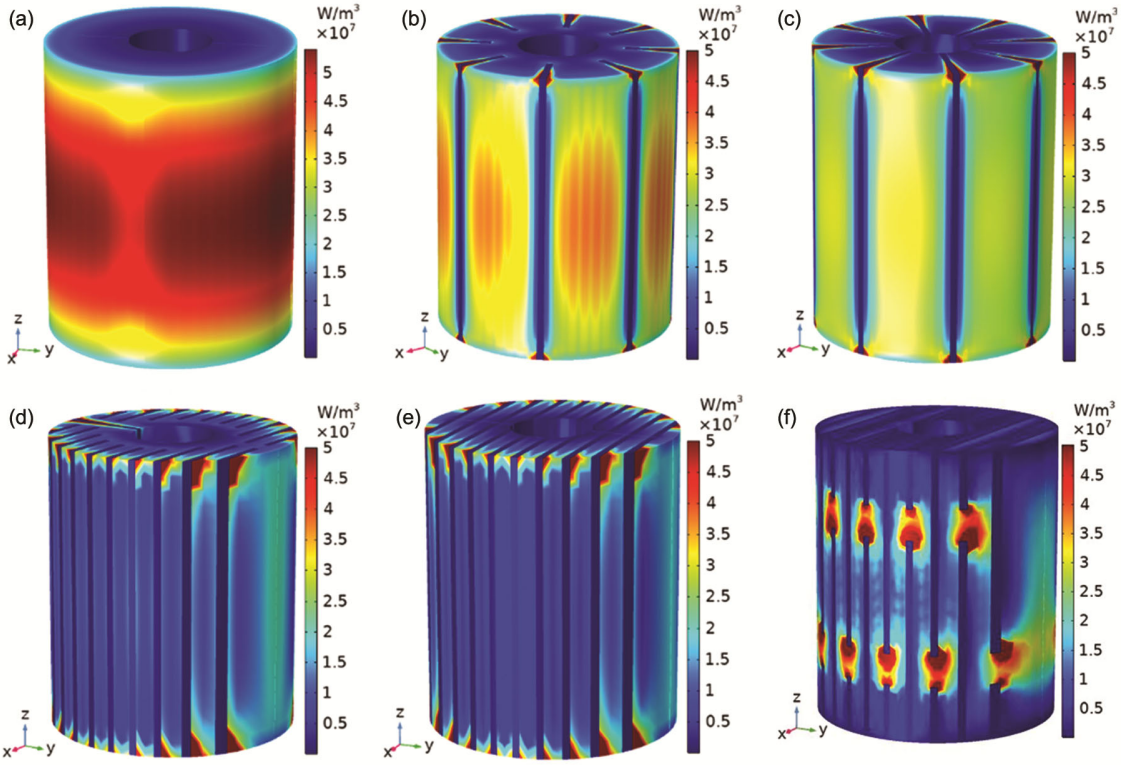

Fig. 5 — Eddy current loss distribution diagram of Terfenol-D rods. (a) Untreated; (b) Radial slit; (c) Radial cut and bonded; (d) Sliced and grooved; (e) Sliced; (f) Sliced at both ends.

surface of the slit and sliced rods significantly reduced compared with the untreated rod (Fig. 4(a)); the hysteresis loss of the outer diameter surface of the sliced rods was less than that of the slit rods; in addition, the sliced Terfenol-D rod at both ends (Fig. 4(f)) had severe hysteresis loss near the connection part between the slices.

Figure 5 shows the eddy current loss distribution of the Terfenol-D rods with different structures. The results suggested that the untreated rod (Fig. 5(a)) had the largest eddy current loss on the outer diameter surface; the eddy current loss on the outer diameter surface of the slit and sliced rods significantly reduced compared with the untreated rod (Fig. 5(a)); the eddy current loss of the outer diameter surface of the sliced rods was smaller than that of the slit rods. The eddy current loss of the slice shape corners and connecting parts between the slices in the sliced rods was large.

The overall hysteresis and eddy current losses of the rods were volume integrated in the derived values of the results in COMSOL Multi physics 5.4 (Fig. 6). Based on this figure, the hysteresis loss of the untreated Terfenol-D rod (Fig. 6(a)) was the smallest; compared with the untreated Terfenol-D rod, the

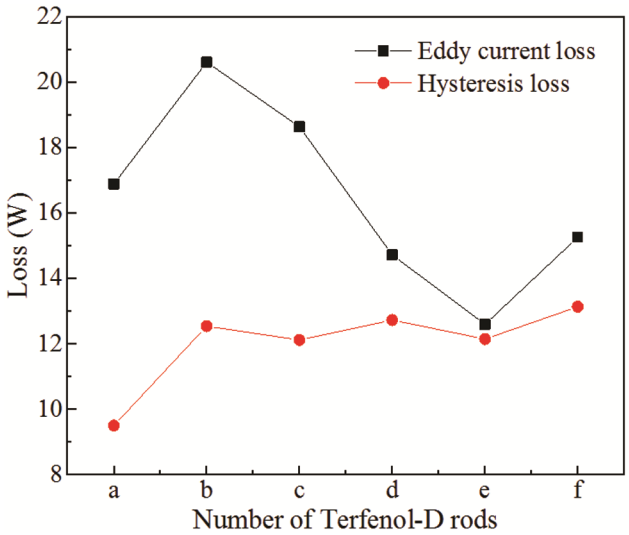

Fig. 6 — Hysteresis loss and eddy current loss of Terfenol-D rods.

hysteresis loss of the slit and sliced Terfenol-D rods increased. Compared with the eddy current loss of the untreated Terfenol-D rod (Fig. 6(a)), the eddy current losses of the sliced rods decreased. But, the eddy current loss of the radially slit (Fig. 5(b)), and radially cut and bonded (Fig. 6(c)) increased. The sliced Terfenol-D rods reduce the cross section of magnetic flux through the rod and the "path" of the eddy

current generated by the magnetic flux. Therefore, the eddy current loss of the rod was reduced. The slitting treatment of the Terfenol-D rods reduced the cross section of the magnetic flux through the rod, but the "path" of the eddy current generated by magnetic flux increased, resulting in higher eddy current losses. The eddy current loss of each Terfenol-D rod was larger than its hysteresis loss.

The loss factor of a ferromagnetic material is the ratio of the magnetic energy lost per period to the magnetic energy stored, which is defined as the ratio of resistance to reactance. It can be calculated as follows:

$$\tan\delta = \frac{R}{\omega L} \qquad ...(3)$$

Where R and L are the resistance and inductance of the excitation coil, respectively

The loss factor is a physical quantity reflecting the intrinsic magnetism of ferromagnetic materials, and a critical indicator for measuring the magnetism of a material; the smaller the loss factor, the less is the loss of magnetic energy.

In the global evaluation of the results in COMSOL Multiphysics 5.4, the coil resistance and inductance of the Terfenol-D rods with different structures were obtained, and the loss factor of the rods was obtained according to equation (3), Fig. 7 shows the loss factors of Terfenol-D rods. The results showed that the Terfenol-D rod with radially slit (Fig. 7(b)) had the largest loss factor, and the core loss was severe; the loss factor of the slit Terfenol-D rods and the untreated Terfenol-D rod (Fig. 7(a)) was larger than

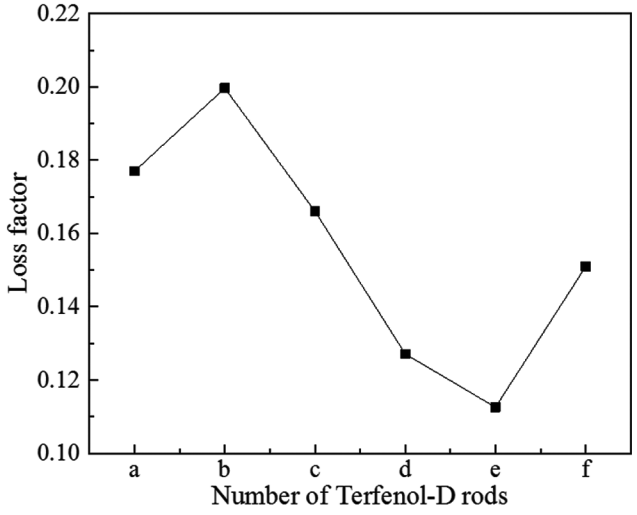

Fig. 7 — Loss factors of Terfenol-D rods.

that of the sliced Terfenol-D rods, suggesting that the core losses could be more effectively reduced by sliced Terfenol-D rods. The slice treatment rod (Fig. 7(e)) had the smallest loss factor and the least core loss among the Terfenol-D rod structures.

During the operation of the giant magnetostrictive transducer, the coil was energized due to a certain resistance of the coil, and the wires in the coil would generate resistance loss.

The theoretical length of the coil can be calculated as follows:

$$l_c = \pi R_1 N(1+\alpha) \qquad ...(4)$$

$$\alpha = \frac{R_2}{R_1} = 2.5 \qquad ... (5)$$

Where R_1 and R_2 are, respectively, the inner and outer diameters of the coil.

The coil resistance calculation formula is expressed as follows:

$$R_c = \rho \frac{l_c}{S} \qquad ...(6)$$

Where ρ and S are the resistivity and cross sectional area of the wire, respectively.

The power loss of the coil resistance is calculated as follows:

$$P_c = I^2 R_c \qquad ...(7)$$

Where I is the excitation current of the coil.

In the derived values of the results in COMSOL Multiphysics 5.4, the coil resistance loss is obtained by volume integration. Table 1 shows the coil resistance losses of Terfenol-D rods with different structures. The coil resistance losses of the untreated rod (a) and radially cut and bonding rod (c) were the same, and the finite element-simulated values were larger than the theoretically calculated values. The radially slit (b), sliced and grooved (d), the sliced (e), and sliced at both ends (f) rods had the same coil resistance loss. The finite element simulation calculation value was less than the theoretical calculation value. The finite element simulation calculation values of the coil resistance losses of the six Terfenol-D rods basically agreed with the theoretical calculation values.

4 Experimental Tests

Three structures of Terfenol-D rods were manufactured: the untreated (a), radially slit (b), and

Table 1 — Coil resistance loss of Terfenol-D rods with different structures.

Structure of Terfenol-D rod	(a) Untreated	(b) Radially slit	(c) Radially cut and bonded	(d) Sliced and grooved	(e) Sliced treatment	(f) Sliced at both ends
Simulation value/W	0.320	0.308	0.320	0.308	0.308	0.308
Theoretical value/W	0.309					

Fig. 8 — Three structures of Terfenol-D rods.

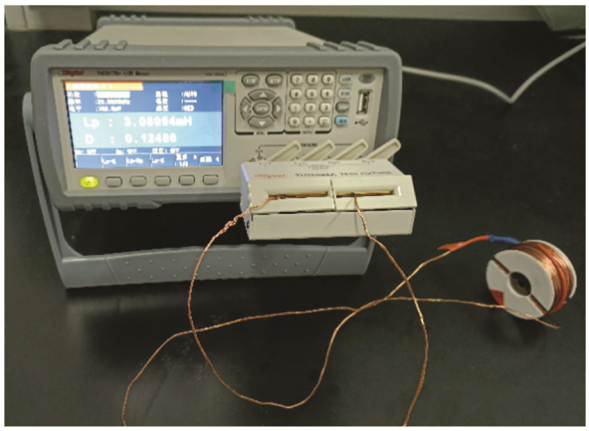

Fig. 9 — Experimental test diagram.

sliced at both ends (f) Terfenol-D rods (Fig. 8). LCR Meter (TH2817B+, Tonghui, China) tested the loss factors of the three structures of Terfenol-D rods at 20 kHz. Fig. 9 shows the experimental test diagram.

Table 2 shows the results of experimental tests and finite element calculations of the loss factors of the Terfenol-D rods. The loss factor of the radially slit rod (b) was the largest, where as that of the sliced rod at both ends (f) was the smallest, which suggests that core losses could be more effectively reduced by sliced Terfenol-D rods.The finite element simulation values of the loss factors of the three structures of Terfenol-D rods basically agreed with the experimental measurements, with some errors. The reason might be that the standard material parameters of the theoretical analysis were not the same as the actual material parameters.

Table 2 — Loss factors of Terfenol-D rods.

Structure of Terfenol-D rod	(a) Untreated	(b) Radially slit	(f) Sliced at both ends
Simulation value	0.177	0.199	0.151
Measured value	0.119	0.124	0.100

5 Conclusions

Six structures of Terfenol-D rods were studied. The hysteresis and eddy current losses of the Terfenol-D rods and resistance loss of the coil were simulated and calculated using COMSOL Multiphysics finite element software, and the loss factors of the rods were calculated. Further, three structures of Terfenol-D rods were manufactured, and their loss factors were tested. The results showed that the untreated rod had the largest hysteresis loss and eddy current loss on the outer diameter surface, and the overall hysteresis loss of the untreated rod was the smallest; compared with the untreated rod, eddy current loss and hysteresis loss on the outer diameter surface of sliced and slit rods reduced, the overall hysteresis loss of sliced and slit rods increased, and the overall eddy current loss of sliced rods reduced, The eddy current loss of the radial slit, and radially cut and bonded increased; the hysteresis and eddy current losses on the surface of the sliced rods were less than those of the slit rod, and the overall eddy current losses of the sliced rods were less than that of the slit rod; the eddy current loss of each rod was larger than its hysteresis loss.

The finite element-simulated values of the coil resistance losses for different structures of Terfenol-D rods basically agreed with the theoretically calculated values. The loss factor of the radially slit Terfenol-D rod was the largest, whereas that of the sliced at both ends Terfenol-D rod was the smallest. The finite element simulation values of the loss factors of the three manufactured Terfenol-D rods agreed with the experimental values. This research contribute to the efficient use of Terfenol-D, which has very important reference and guiding significance for the design of high-power ultrasonic vibration system.

Declaration of Competing Interest

The authors declare that they have no known competing financial interests or personal relationships

that could have appeared to influence the work reported in this paper.

Acknowledgements

This work was supported by the National Natural Science Foundation of China (No. 12174241), and the Fundamental Research Funds for the Central Universities (No. 2020TS024).

References

1 YaoY, PanY & Liu S,*Ultrason Sonochem*, 62 (2020) 104722.
2 Li P, Chen Y, Li W, *et al*., *Alexandria Eng J*, 61 (2022) 10939.
3 Pernía A M, Mayor H A, Prieto M J, *et al*., *Sensors*, 19 (2019) 2382.
4 Tang J, Bai Y, Yan L, *et al*., *Appl Acoust*, 190 (2022) 108646.
5 Liu H, Li W, Sun X,*et al., J Sound Vib*, 492 (2020) 115805.
6 Kwak Y, Kim S, Ahn J, *Int J Precis Eng Man*, 12 (2011) 829.
7 Zeng J, Zeng H, Bai B, *et al*., *Proc SPIE 7493, Second International Conference on Smart Materials and Nanotechnology in Engineering*, Weihai, (2009).
8 Takahashi R, Moongki C, Tashiro K, *et al*., *Appl Environ Microb*, 19 (2011) 503.
9 Engdahl G & Bergqvist A, *J Appl Phys*, 79 (1996) 4689.
10 Xu H, Pei Y, Fang D, *et al*., *Int J Solids Struct*, 50 (2013) 672.
11 Talebian S, Hojjat Y, Ghodsi M, *et al*., *J Magn Magn Mater*, 388 (2015) 150.
12 Yamamoto K, Nakano H, Yamashiro Y, *J Magn Magn Mater*, 254 (2003) 222.
13 Meng H, Zhang T, Jiang C, *IEEE T Magn*, 50 (2014) 1.
14 Stillesjo F, Engdahl G, Wei Z, *Proc SPIE 3992, Smart Structures and Materials*, California, (2000).
15 Huang W, Gao C,Li Y, *et al*., *IEEE Trans Magn*, 54(2018) 1.
16 He X & Zhang P, *Sci China: Technol Sci*, 52 (2009) 336.
17 Tang Z, Lv F & Liu Y, *J Rare Earths*, 27 (2009) 525.
18 Teng D & Li Y, *Sensors*, 20 (2020) 2808.
19 Tao M, Chen D, Lu Q, *et al.*, *J Mech Eng*, 48 (2012) 146.
20 Gandomzadeh D & Abbaspour-Fard M, *J Magn Magn Mater*, 513 (2020) 166823.
21 Huang W, Wu X & Guo P, *IEEE Trans Magn*, 57 (2021) 1.
22 Li P, Liu Q, Zhou X, *et al*., *J Vib Control*, 27 (2020) 573.
23 AC/DC Module User's Guide. COMSOL Multiphysics® V-5.4. COMSOL AB, Stockholm, (2018).
24 Huang W, Wu X, Wu Y, *et al*., *Chin J Sci Instrum*, 41 (2020) 215.